# Solid-liquid Two Phase Flow Simulation on Particle Motion in the Axial Flow Pump

Zhipeng Chen, Kun Hu\*

Mechanical and Electrical Engineering College, Southwest Petroleum University, Chengdu 610000, China

#### **Abstract**

Based on the DEM-CFD method, the solid-liquid two-phase flow in an axial flow pump was simulated, and the velocity and trajectory of particles passing through the impeller and deflector were investigated. It was found that the particles accelerated about 150% after passing through the impeller. Five solid concentration schemes were set up to explore the influence of solid concentration on particle velocity and average residence time. The maximum velocity of particles at different concentrations tended to 10 m/s; The average residence time of particles in low concentration scheme (2%) is 120% of that in other schemes. The research in this paper can be used as a reference to reduce the erosion wear in the pump and enhance the heat transfer effect.

## **Keywords**

DEM-CFD; Axial Flow Pump; Particle Trajectory; Particle Residence Time.

#### 1. Introduction

The study of solid-liquid two-phase flow in the pump can provide reference for reducing the wear of the flow passage components and improving the hydraulic performance.

In recent years, scholars have carried out internal flow analysis of axial flow pump based on CFD software. based on large eddy simulation, Kan K [1] et al. simulated the kinetic energy dissipation and flow structure of water flowing through the axial flow pump under different flow conditions. The research results showed that the high intensity of turbulent kinetic energy caused unstable shock wave and top gap leakage. Based on two different streamline design methods, Zhang Xiaodong [2] et al simulated the solid-liquid two-phase flow of the φ79 mm solid-liquid axial flow pump, it was found that the axial flow pump designed based on the streamline method was more suitable for the actual requirements of mining. Wu Likun [3] carried out solid-liquid two-phase simulation of water-jet propulsion axial flow pump and found that under the action of low particle concentration of sand water, particle concentration has limited impact on the pump characteristics. Wang Yiran [4] carried out the internal flow analysis of the pump to optimize the performance of the annular axial flow pump in the propylene synthesis process, and found that the SST model was the most suitable turbulence model for the flow field calculation of rotating machinery. Lang Tao [5] et al. carried out solidliquid two-phase numerical simulation based on the Particle model and found that the swept angle of the blade had an impact on the pump lifting and winding performance. When the axial flow pump is conveying the flow with sand, the particles are affected by the flow field of the impeller and the deflector, which makes it difficult for the current CFD method to predict the movement of particles in the pump.

Based on the DEM-CFD method, this paper considers the interaction between particles, between particles and wall, to explore the motion law of particles.

## 2. DEM(Discrete Element Method) Theory.

#### 2.1. Normal Force Contact Model

Walton and Braun [6] proposed a Hysteretic linear spring model based on the elastoplastic theory to describe the normal repulsive force and energy dissipation when particles interact with each other. This method can ignore the viscous damping term and make the energy dissipation insensitive to the contact in the non-direction. The model is described as follows:

$$F_{n} = \begin{cases} \min\left(\mathbf{K}_{nl}S_{n}^{t}, F_{n}^{t-\Delta t} + \mathbf{K}_{nu}\Delta S_{n}\right) \\ \max\left(F_{n}^{t-\Delta t} + \mathbf{K}_{nu}\Delta S_{n}, \lambda \mathbf{K}_{nl}S_{n}^{t}\right) \end{cases}$$

Where:  $F^{t_n}$  and  $F^{t-\Delta t}$  - $\Delta t$  are the normal contact force at the time of t and t- $\Delta t$ , N;  $\Delta T$ -time step, s;  $\Delta S^{n-1}$  overlapping distance between particles, mm;  $K_{nl}$  and  $K_{nu}$  are the contact stiffness coefficients during loading and unloading respectively.

## 2.2. Tangential Force Contact Model.

The Coulomb limit model assumes that the tangential component of relative velocity is the cause of sliding displacement. The model is described as follows:

$$F_{\tau} = -\mu F_n \frac{\mathbf{s}_{\tau}}{|\mathbf{s}_{\tau}|}$$

Where:  $\mu$ - Friction coefficient;  $\mu_m$ -sliding friction coefficient;  $\mu_s$ -Static friction coefficient without sliding;  $F_n$  - normal contact force, N;  $s_{\tau}$  is the tangential vector of relative velocity.

### 2.3. Rolling Resistance Model.

The constant resistance model applies a constant resistance moment  $M_r$  to the particles:

$$M_{r} = -\mu_{r} |\mathbf{r}| F_{n} \frac{\omega}{|\omega|}$$

Where:  $\mu_r$  - rolling resistance coefficient [7];  $F_n$  - normal contact force, N;  $\omega$ - Angular velocity vector of particles; r - rolling radius of particles, mm.

#### 3. Calculation Model

This paper uses CFturbo software to bu axial flow pump, and the hydraulic parameters of the pump are shown in Table 1; The mesh of the pump is shown in Figure 1.



Fig 1. Grid diagram

Table 1. Hydraulic parameters of pump

| Head | Flow       | R speed                  | Number of blades |
|------|------------|--------------------------|------------------|
| H/m  | Q/(m³•s-1) | n/(r•min <sup>-1</sup> ) |                  |
| 5.30 | 21.25      | 150                      | 4                |

## 4. Solid-liquid Two-phase Calculation.

## 4.1. Boundary Condition Settings.

FLUENT performs the transient calculation based on the pressure solver and opens the slip grid equation to make the impeller region rotate relatively at the speed of 150r/min<sup>-1</sup>; Turbulence model select SST k-  $\omega$  Model; Set the speed inlet condition and pressure outlet condition, and set the time step to  $1\times10^{-4}$ s. The particles in DEM are continuously injected at the inlet of the particle setting, with a time step of  $5\times10^{-6}$ s

## 4.2. Grid Independence Analysis.

Table 2. Grid Scheme

| Grid Scheme     | a                  | b                    | С                     | d                      | e                       |
|-----------------|--------------------|----------------------|-----------------------|------------------------|-------------------------|
| Number of grids | 1×10 <sup>-6</sup> | 1.2×10 <sup>-6</sup> | 1.44×10 <sup>-6</sup> | 1.728×10 <sup>-6</sup> | 2.0736×10 <sup>-6</sup> |
| H/m             | 5.19               | 5.29                 | 5.52                  | 5.31                   | 5.28                    |

In order to verify the independence of the simulation results and the number of grids, five groups of grids with the number increasing by 20% are generated, and the coupling calculation is carried out respectively, and the residuals are converged to  $1 \times 10^{-3}$ , until the inlet flow is no longer changed, the head H is shown in Table 2. It can be seen that the number of meshes has little influence on the simulation results. In order to save computing resources, 144W grid is selected for numerical research.

# 5. Analysis of Calculation Results.

In order to study the effect of solid concentration on particle motion, different solid (volume percentage) concentrations are set under the design condition  $Q=21.25\,\text{m}^3/\text{s}$ , as shown in Table 3.

**Table 3.** Simulation scheme of the influence of solid concentration

| scheme        | I  | II | III | IV | V   |
|---------------|----|----|-----|----|-----|
| concentration | 2% | 4% | 6%  | 8% | 10% |

#### **5.1.** Particle Trajectory Analysis

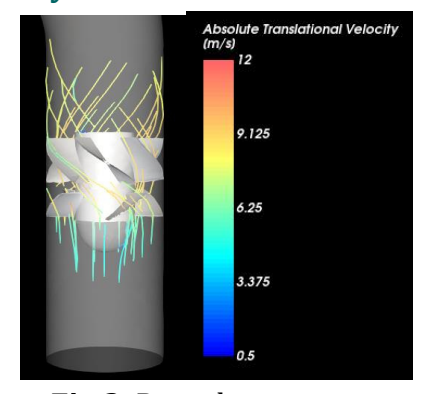


Fig 2. Particle trajectory

The particle motion trajectory is shown in Figure 2. When entering the impeller area, the particle velocity is lower than 6.25m/s. After entering the impeller, the particle flows in the direction of impeller rotation and accelerates to about 9.125m/s. When the particle passes through the deflector, the velocity remains unchanged, and the particle moves close to the wall;

#### **5.2.** Particle Velocity Analysis.

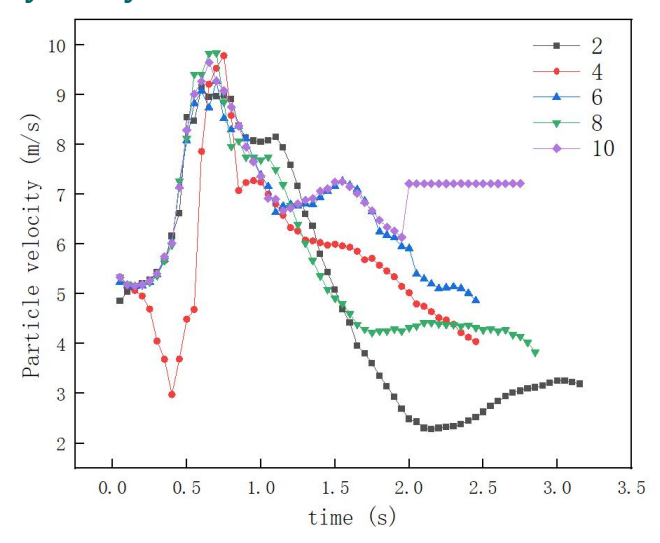


Fig 3. Effect of solid concentration on particle velocity

Marking the same particle (id=10) at the inlet, the effect of solid concentration on particle velocity under five calculation schemes is shown in Figure 3,It can be seen that the change of particle velocity with solid concentration is basically the same, the particles accelerate and reach the peak in the range of t=0.5-0.8s,the maximum speed of the five schemes is close to 10m/s; After passing through this area, the speed starts to drop sharply, and after t=2.0s, the speed area is fixed in a gentle area, In general, the higher the solid concentration, the greater the final speed. It can be seen that the particles pass through the impeller area at 0.5s-0.8s, and the speed at different concentrations is the highest after the particles lose power, resulting in the reduction of kinetic energy.

#### **5.3.** Particle Residence Time Analysis.

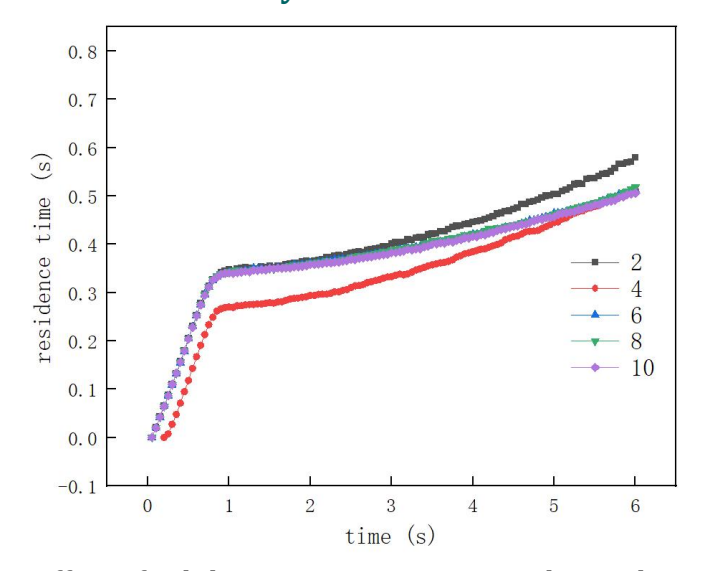


Fig 4. Effect of solid concentration on particle residence time

Figure 4 shows the average residence time of all particles in the impeller and deflector area. Under different calculation schemes, the change trend of the average residence time of particles is consistent. At 0s-1s after the axial flow pump is just started, the particles began to fill this area rapidly, and the residence time showed a rapid upward trend; After 1 s, the particles in the region are completely filled, the internal flow field tends to be stable, and the residence time is slowly rising; The final residence time of Scheme II-V tends to be consistent around 0.5s, while the final residence time of scheme I is about 0.6s; It can be seen that at low concentration (2%), the retention effect of particles is the most obvious, and the effect of stirring and heat transfer is the most effective.

# 6. Summary

- 1. When particles flow through the impeller area, they will erode the impeller area, while when particles flow through the deflector, the erosion effect is small.
- 2. At low concentration (2%), the retention effect of particles is the most obvious, and the effect of stirring and heat transfer is the best.

#### References

- [1] Kan K, Yang ZX, Pin Lyu et al. Numerical study of turbulent flow past a rotating axial-flow pump based on a level-set immersed boundary method. [J] Renewable Energy 168, pp.960-971.
- [2] Zhang XiaoDong, Hao renjie, Gong yan et al. Blade design and analysis of solid-liquid mixed axial flow pump[J]. Petroleum machinery. Vol 48(2020).90-97.
- [3] Wu LiKun. Study on solid-liquid two-phase flow of water jet propulsion pump[D]. Hefei University of Technology, 2020.
- [4] Wang yiran. Study on Solid-liquid Two-phase Flow of Polypropylene Annular Axial Flow Pump [D]. Hefei University of Technology, 2019.
- [5] Lang Tao, Shi Wei Dong, Xie Jing et al. Solid-liquid two-phase distribution and winding test of swept axial flow pump with the same external characteristics[J]. Journal of Agricultural Engineering. Vol31 (2015), p.42-50.
- [6] Walton, O. R. and Braun, R. L. Viscosity, granular-temperature, and stress calculations for shearing assemblies of inelastic, frictional disks. Journal of Rheology[J], 1986, 30: pp.948–980.
- [7] Jun Ai, Jian-Fei Chen, J. Michael Rotter, et al. Assessment of rolling resistance models in discrete element simulations[J]. Powder Technology, 2010, pp.206(3).